Effects of the spin-orbit interaction in Heusler compounds: Electronic structures and Fermi surfaces of NiMnSb and PtMnSb

S. J. Youn and B. I. Min
Department of Physics, Pohang University of Science and Technology, Pohang 790-784, Korea
(Received 30 November 1994)

Electronic structures of the Heusler compounds, NiMnSb and PtMnSb, are investigated by using the linearized-muffin-tin-orbital band method. Equilibrium properties such as lattice constants and bulk moduli are obtained from total energy calculations and effects of the spin-orbit interaction on electronic structures and Fermi surfaces are explored. In the semirelativistic band calculations, NiMnSb is half-metallic, i.e., metallic for majority spin while semiconducting for minority spin bands, but PtMnSb is normal metallic at the experimental lattice constant. PtMnSb becomes a half metal if we take into account the spin-orbit interaction explicitly in the calculation. Equilibrium lattice constants obtained in the ferromagnetic band calculations agree very well with experimental values. The magnitudes of the energy gap in the minority spin bands are found to be sensitive to the variation of the lattice constants for NiMnSb and PtMnSb. The effect of the spin-orbit interaction is substantial in PtMnSb, in contrast to NiMnSb in which it is negligible. A large spin-orbit splitting at Γ in PtMnSb is due to Pt $6p$ states near E_F, which may be involved in optical transitions to generate a large magneto-optical Kerr effect. Further, the itinerant electrons that mediate the Ruderman-Kittel-Kasuya-Yosida interaction between Mn magnetic moments in NiMnSb and PtMnSb are identified as those on the nearly spherical hole Fermi surfaces of the 12th majority spin bands centered at Γ.

I. INTRODUCTION

Heusler compounds of XMnY type have recently attracted attention since de Groot *et al.*[1] predicted that NiMnSb and PtMnSb are half-metallic ferromagnets, i.e., the majority spin bands are metallic, while the minority spin bands are semiconducting. The conduction electrons at the Fermi level E_F are 100% spin-polarized, which suggests that these materials can be used as spin-polarized electron sources. Furthermore, PtMnSb exhibits a very large magneto-optical Kerr effect (MOKE),[2] which will be very useful for the application as an erasable optical memory device.

There exist several electronic structure studies for these materials. Using the concept of the spin-orbit splitting of energy bands near E_F, de Groot *et al.*[3,4] have provided a qualitative explanation for the large MOKE observed in PtMnSb. The spin-orbit interaction, however, was not included in their augmented spherical wave band calculations. By employing the non-self-consistent Korringa-Kohn-Rostoker (KKR) band method, Hanssen and Mijnarends[5] obtained a half-metallic band for NiMnSb at the experimental lattice constant. They presented the Fermi surface and the momentum density of annihilation photon pairs. Kulatov and Mazin[6] also obtained a half-metallic band for NiMnSb at the experimental lattice constant by using the linearized-muffin-tin-orbital (LMTO) band method, and showed that the position of E_F with respect to the band gap is quite sensitive to exchange-correlation potentials employed in calculations. In previous calculations, however, no attempts have been made to explore the total energy equilibrium properties or the effect of the spin-orbit interaction.

The motivation of this work is to study the effect of spin-orbit interaction on the electronic structures of NiMnSb and PtMnSb. We have performed total energy local spin density functional LMTO band structure calculations on NiMnSb and PtMnSb, and investigated the equilibrium properties such as lattice constant and bulk modulus. In order to examine the spin-orbit effect on the band structures and Fermi surfaces, we have carried out band calculations taking into account explicitly the spin-orbit interaction and compared them with conventional semirelativistic spin-polarized band calculations.

Our paper is organized as follows. In Sec. II, computational methods and the crystal structure of the Heusler compounds are described. Results for NiMnSb and PtMnSb are presented in Sec. III and Sec. IV, respectively. The final conclusion follows in Sec. VI.

II. COMPUTATIONAL DETAILS

Band structures are obtained by using the self-consistent LMTO band method with an atomic sphere approximation.[7] Electronic wave functions of all atoms in the unit cell were expanded by utilizing basis functions up to d orbitals. We have assumed that all atoms have the same Wigner-Seitz radii.[9] The von Barth-Hedin form of exchange-correlation potential[8] is utilized and the density of state (DOS) is calculated using the linear tetrahedron method.[10] A convergence test of the total energy with respect to the number of $\vec{k}$ points indicates that a sampling of 90 $\vec{k}$ points in an irreducible Bril-

louin zone is sufficient to get the energy precision of 1 m Ry, and thus we have used 90 $\vec{k}$ points for the $\vec{k}$-space integrals in all the calculations. The computational implementations of the spin-orbit interaction Hamiltonian in our band calculation are described in Refs. 7 and 11.

A general formula unit of the Heusler compounds is X_nMnY with $n = 1$ or 2, where X denotes a transition metal and Y denotes an s-p element such as Al, Sb, and Sn. The original material reported by Heusler was Cu_2MnAl.[12] The unit cell of X_2MnY type is a face centered cubic with four basis atoms. Coordinates of the basis atoms are $X_1(0,0,0)$, Mn$(\frac{1}{4},\frac{1}{4},\frac{1}{4})$, $X_2(\frac{1}{2},\frac{1}{2},\frac{1}{2})$, and $Y(\frac{3}{4},\frac{3}{4},\frac{3}{4})$, respectively. Both NiMnSb and PtMnSb correspond to the XMnY type (C_{1b} structure or MgAgAs structure with the space group T_d^2), where the $X_2(\frac{1}{2},\frac{1}{2},\frac{1}{2})$ sites in the unit cell of X_2MnY are empty.[13] Hence the $X_2(\frac{1}{2},\frac{1}{2},\frac{1}{2})$ sites are treated as an empty sphere in our calculation.

III. ELECTRONIC STRUCTURES OF NiMnSb

We have performed total energy calculations for both paramagnetic and ferromagnetic phases of NiMnSb. Results of equilibrium lattice constants and bulk moduli are summarized in Table I. As is well known, the equilibrium lattice constant obtained from the paramagnetic calculation is much smaller than the experimental one, while the ferromagnetic calculation yields an expanded equilibrium lattice constant. The calculated equilibrium lattice constants of NiMnSb (5.77 Å and 5.90 Å for the paramagnetic and ferromagnetic phase, respectively) follow this tendency. The equilibrium lattice constant obtained from the ferromagnetic calculation agrees very well with the experimental lattice constant ($\sim$ 0.3% error). We found from total energy calculations that the inclusion of the Sb-d orbital is crucial in the LMTO calculation for NiMnSb. Without the Sb-d orbital, we obtained an equilibrium lattice constant (6.07 Å), which is larger than the experimental one by $\sim$ 2.7%.

The Stoner factor, defined as $N(E_F)I_{xc}$ where $N(E_F)$ is the paramagnetic density of states at E_F and I_{xc} is the intra-atomic exchange correlation integral, is 4×10^{-5} (< 1.0). It implies that there is no ferromagnetic instability in the framework of the Stoner theory of magnetism.[14] In reality, the ferromagnetic phase of NiMnSb is more stable than the paramagnetic one, which indicates that the conventional Stoner theory is not applicable to NiMnSb. As pointed out by Kulatov and Mazin,[6] the small Stoner factor is due to the very small value of DOS at E_F (nearly zero) in the paramagnetic phase of NiMnSb. By using the extended version of the Stoner theory, they accounted for the ferromagnetic instability of NiMnSb correctly.

Spin-polarized band structures of NiMnSb, calculated at the experimental lattice constant, are presented in Fig. 1. The band structure in Fig. 1(a) is obtained semirelativistically including all the relativistic effects but the spin-orbit interaction, while the band structure in Fig. 1(b) is obtained with the spin-orbit interaction incorporated. In Fig. 1(a), solid lines and dotted lines represent majority spin-up and minority spin-down bands, respectively. The lowest band located at about 12 eV below E_F with mainly Sb-5s character is not shown in Fig. 1. The present band structure in Fig. 1(a) is essentially identical to that of de Groot *et al.*,[1] and it reveals the half-metallic character of NiMnSb very well. The Fermi level cuts the majority spin-up bands, which is characteristic of a metallic band, whereas it lies in the gap of minority spin-down bands, reflecting a semiconducting behavior. The energy gap in minority spin-down bands is between the 9th band at Γ and the 10th band at X, which is indirect with a size of 0.55 eV. The observed onset energy of interband optical transition in NiMnSb is thought to correspond to this indirect energy gap.[15] Meanwhile, the direct energy gap at Γ is 1.89 eV.

Once the spin-orbit interaction is included, the indirect gap becomes wider by $\sim$ 0.06 eV (see Table II). However, the band structure of Fig. 1(b), with the spin-orbit interaction included, is nearly the same as the semirelativistic band structure of Fig. 1(a), suggesting that the effect of the spin-orbit interaction on the overall band structure of NiMnSb is small. The magnitude of spin-orbit splitting is only $\sim$ 0.02 eV for the triply degenerate spin-down bands at Γ (7, 8, and 9th bands), which are composed of Mn 3d and Ni 4p states.

Total and projected local densities of state (PLDOS's) of ferromagnetic NiMnSb obtained with the spin-orbit interaction included are shown in Fig. 2. The gap in the minority spin-down band is clearly seen in Fig. 2(a), where E_F is located near the conduction band edge. The Mn-3d PLDOS consists of three main peaks at -2.9 eV, -1.3 eV, and 1.2 eV. The peak at 1.2 eV results from the exchange interaction between 3d electrons, which gives rise to a large magnetic moment at Mn sites. The energy range of the Ni-3d PLDOS is nearly the same as that of the Mn-3d PLDOS, while the Sb-5p PLDOS is located at lower energies than the Ni or Mn PLDOS's. Calculated

TABLE I. Equilibrium properties of NiMnSb and PtMnSb. Calculated equilibrium lattice constants (a_{cal}), experimental lattice constants (a_{exp}), and calculated bulk moduli (B_{cal}) from paramagnetic (P) and ferromagnetic (F) calculations.

	NiMnSb		PtMnSb	
	Paramagnetic	Ferromagnetic	Paramagnetic	Ferromagnetic
a_{cal} (Å)	5.77	5.90	6.15	6.24
a_{exp} (Å)		5.92[a]		6.21[a]
B_{cal} (Mbar)	0.42	0.32	0.39	0.33

[a]Reference 2.

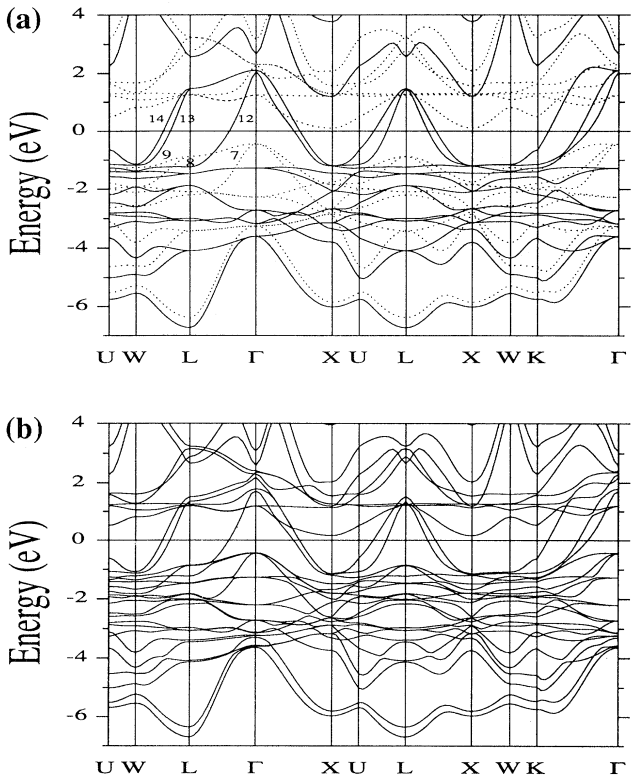

FIG. 1. Band structures of NiMnSb calculated at the experimental lattice constant. The Fermi energy is set to zero. (a) Semirelativistic bands. The first lowest bands in both spin directions are not shown. Solid lines represent spin-up bands and dotted lines represent spin-down bands. The top of the minority spin valence band corresponds to the 9th band, and the bottom of conduction band corresponds to the 10th band. (b) Bands with the spin-orbit interaction included.

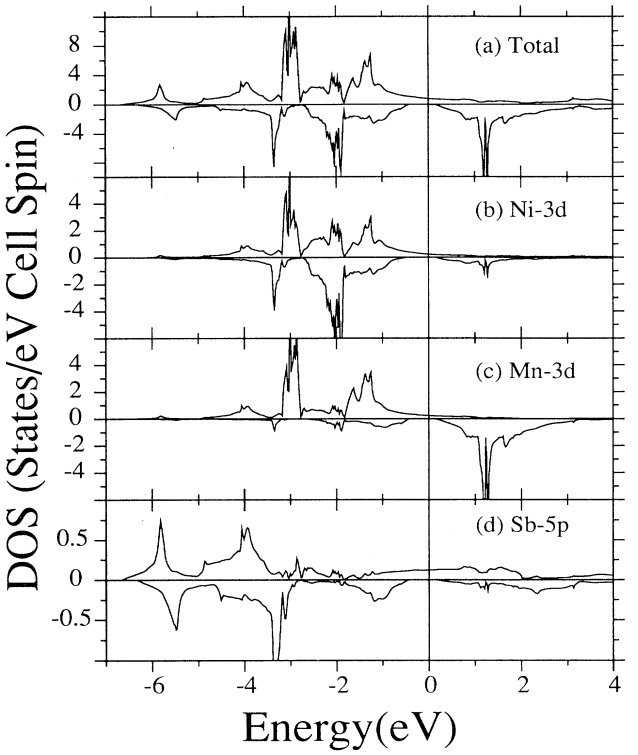

FIG. 2. The total DOS (states/eV spin cell) and PLDOS's (states/eV spin atom) of NiMnSb calculated at the experimental lattice constant. (a) Total DOS, (b) PLDOS of Mn-3d, (c) PLDOS of Ni-3d, and (d) PLDOS of Sb-5p.

PLDOS's are qualitatively consistent with experimental results of the photoemission spectroscopy.[16] However, discrepancies exist in the location and the width of the peaks between theory and experiment, which may be due to the matrix element and relaxation effects in the photoionization process, and large correlation effects among 3d electrons of Mn and Ni atoms. The exchange splitting of Mn-3d band yields a large magnetic moment, $3.76\mu_B$ per Mn atom (see Table III). In contrast, Ni-3d bands are evenly filled with electrons from both spins, and so the magnetic moment at Ni is as small as $0.26\mu_B$. Considering that the total magnetic moment of NiMnSb is $4.0\mu_B$ per formula unit, the magnetic moment is carried mainly by Mn atoms. The calculated total moment is in agreement with previous calculations and experiments.[17,18] Note that, in the case of half-metallic NiMnSb 9 out of total 22 electrons are occupied in spin-down bands, and so the total spin magnetic moment of NiMnSb becomes exactly $4.0\mu_B$.

Figures 3(a) and 3(b) present calculated Fermi surfaces of NiMnSb without and with the effect of the spin-orbit interaction included, respectively. The shape of Fermi surfaces obtained with the effect of spin-orbit interaction included are very similar to that of the semirelativistic

TABLE II. Calculated energy gaps in minority spin bands. S.R represents the semirelativistic calculation and S.R+S.O. represents a calculation with the spin-orbit interaction included. The onset of observed interband transitions are also provided for comparison.

	NiMnSb		PtMnSb	
	S.R	S.R+S.O	S.R	S.R+S.O
$\Delta E(\Gamma - X)$ (eV)	0.55	0.61	1.11	0.91
$\Delta E(\Gamma - \Gamma)$ (eV)	1.89	1.63	1.39	1.38
E(onset) (eV)		0.70[a]		0.90[a]

[a]Reference 15.

TABLE III. Occupied charges, Q_l, and magnetic moments, M, of ferromagnetic NiMnSb at the experimental lattice constant. The spin-orbit interaction is taken into account.

		Q_s	Q_p	Q_d	Q_{tot}	M
Ni	↑	0.36	0.47	4.58	5.41	
	↓	0.38	0.53	4.25	5.16	0.25
Mn	↑	0.29	0.29	4.58	5.16	
	↓	0.24	0.26	0.90	1.40	3.76
Sb	↑	0.71	0.99	0.10	1.81	
	↓	0.70	1.08	0.10	1.88	−0.07
Empty	↑	0.22	0.29	0.12	0.62	
	↓	0.21	0.26	0.10	0.57	0.05

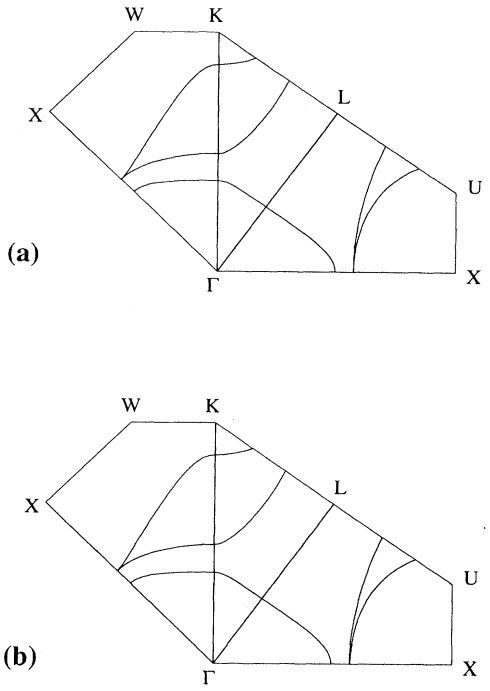

FIG. 3. Fermi surface cross sections of NiMnSb at the experimental lattice constant. (a) Semirelativistic calculation. (b) Fermi surfaces with the spin-orbit interaction included.

Fermi surfaces, as expected from negligible changes observed in the band structure. The overall shapes of Fermi surfaces are in agreement with those of the previous calculation, which used the non-self-consistent KKR band method, and did not include the spin-orbit interaction.[5] Fermi surfaces consist of only spin-up bands because of the half-metallic character. Band indices of Fermi surfaces are 12, 13, and 14, respectively, in order of distance from Γ. The 12th band constitutes a nearly spherical hole pocket around Γ. There are arms along the Γ-L direction, which are attributed to the 13th and 14th bands. These arms may provide open orbits, which can be checked by the magnetoresistance measurement.

IV. ELECTRONIC STRUCTURES OF PtMnSb

Equilibrium lattice constants of PtMnSb obtained from paramagnetic and ferromagnetic calculations, are 6.15 Å and 6.24 Å, respectively. As in NiMnSb, the calculated lattice constant of ferromagnetic PtMnSb is nearly the same as the experimental one with an error less than 0.5% (see Table I). Unlike the case of NiMnSb, the Stoner factor is $N(E_F)I_{xc} = 5.98$ (> 1.0), which predicts well a ferromagnetic instability in PtMnSb.

Figure 4(a) and Fig. 4(b) present band structures of PtMnSb calculated at the experimental lattice constant without and with the spin-orbit interaction included, respectively. The semirelativistic band structure in Fig. 4(a) is normal metallic, since both majority and minority spin bands cross E_F. This result is different from that of de Groot *et al.*[1] who reported that PtMnSb

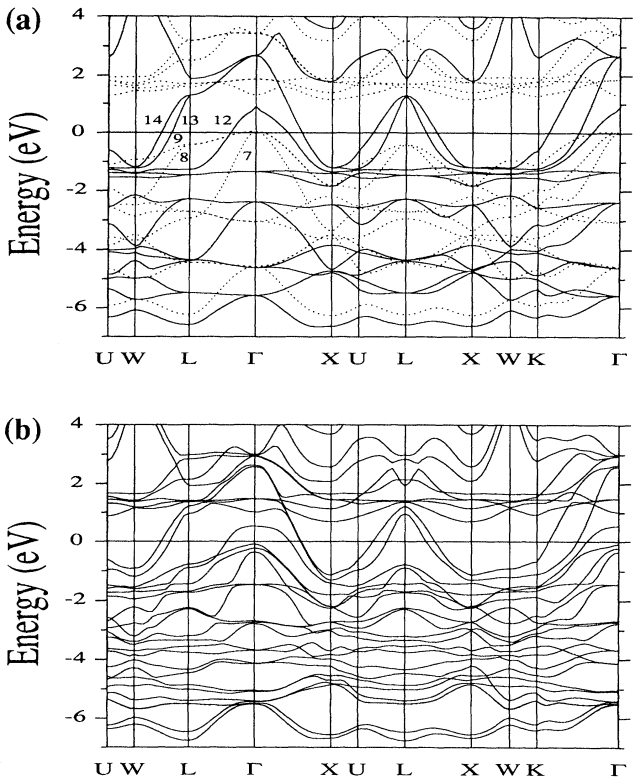

FIG. 4. Band structures of PtMnSb calculated at the experimental lattice constant. (a) Semirelativistic bands. The first lowest bands in both spin directions are omitted. Solid lines represent spin-up bands and dotted lines represent spin-down bands. (b) Bands with spin-orbit interaction included. The first two lowest bands are omitted.

is half-metallic at the experimental lattice constant. The disagreement may be ascribed to the differences in the calculational methods and the types of the exchange-correlation interaction employed.[19] In fact, PtMnSb becomes a half-metal if the spin-orbit interaction is taken into account, as will be discussed below.

Figure 4(b) shows the modified band structure due to the spin-orbit interaction. It is natural to expect that the effect of the spin-orbit interaction is large in PtMnSb, as compared to the case of NiMnSb, due to a large atomic number of Pt. Three degenerate spin-down bands at Γ, which were all above E_F in the semirelativistic calculation, are split into three bands when the spin-orbit interaction is taken into account. Furthermore, all the three split bands are now below E_F so as to make PtMnSb a half metal. The gap in the minority spin band is indirect between Γ and X with a size of 0.91 eV, while the direct energy gap at Γ is 1.38 eV (see Table II). The spin-orbit energy splitting amounts to ~ 0.14 eV, which is 7 times larger than that of NiMnSb, suggesting that the large spin-orbit splitting in PtMnSb originates from Pt atoms. The minority spin bands of PtMnSb at Γ near E_F are composed of 70% Mn-3d, 14% Pt-6p, and 3% Sb-5p states. Note that the Pt-6p character predominates over Sb-5p character in PtMnSb, and so the large spin-orbit splitting of the bands near E_F is ascribed to Pt-6p

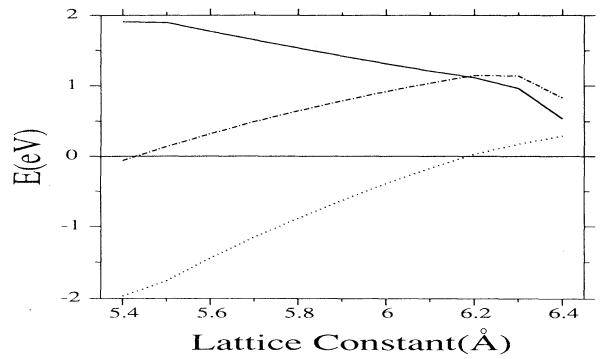

FIG. 5. Energy gap (solid line) in PtMnSb between the 9th and the 10th band vs lattice constant. The Fermi energy is set to zero. The maximum of the 9th band and the minimum of the 10th band are represented by dotted and dot-dashed lines, respectively. The cusp in the variation of the 10th band is due to the change of the minimum energy point, from X to Γ.

bands. This finding is contrary to the report by de Groot *et al.*,[3] in which the states at the top of the valence band have been ascribed to primarily Sb-5p states.

It is pointed out that the enhanced MOKE in PtMnSb is related to an exotic spin-orbit splitting of the minority spin bands at Γ near E_F.[3,4] In this case, the topmost band (9th band) out of three is located above E_F, while the rest two (7th and 8th bands) are below E_F. Then the transition from the empty 9th band to higher 10th or 11th spin-down band at Γ is not possible, and so an incomplete cancellation between transitions of left and right polarized light occurs so as to yield an enhanced optical absorption.[20] Our results do not exhibit such an exotic spin-orbit splitting, since all the three spin-orbit split bands at Γ are below E_F. Nevertheless it is interesting to note that this kind of situation can be realized by shifting down the Fermi level by only ~ 0.1 eV. The 9th band is located only 0.09 eV below E_F. Since the position of E_F is quite sensitive to the employed exchange-correlation potentials, the above condition can be met. This is in contrast to the case in NiMnSb, where the 9th band is located far below E_F (~ 1.0 eV). This unique feature in PtMnSb gives evidence that the spin-orbit split Pt-6p states near E_F, which have minority spin characters, are involved in optical transitions to generate a large MOKE.

The size of the energy gap of the minority spin band depends on the lattice constant very much. Figure 5 shows energy variations of the 9th band maximum and the 10th band minimum of the minority spin band as a function of lattice constant. These values are obtained from the semirelativistic calculations. Dotted and dot-dashed lines represent the 9th band maximum and the 10th minimum, respectively. The solid line represents the difference between these two values, which corresponds to the energy gap. The 9th band maximum is located at Γ, while the location of the 10th band minimum changes from X to Γ with increasing the lattice constant. The half-metallic behavior will be seen in the region, where the 9th band maximum is below E_F, and the 10th band minimum remains above E_F. This figure shows that, as the lattice constant of PtMnSb increases from $a = 5.40$ Å, the energy gap opens in the minority spin band between the 9th and the 10th band, and it becomes a half-metal at $a = 5.46$ Å. As the lattice constant increases further, the 9th band becomes higher in energy crossing E_F at Γ, and PtMnSb becomes a normal metal again. Thus the range of the lattice constant, in which PtMnSb is half-metallic, is between 5.46 Å and 6.18 Å.[21] In this half-metallic region, the total magnetic moment per formula unit has a fixed value, $4.0\mu_B$, and does not change. Since both experimental and calculated lattice constants of PtMnSb are off the half-metallic range, PtMnSb is not half-metallic in the semi-relativistic calculation.

Figure 6 shows the total DOS and PLDOS's of PtMnSb, calculated at the experimental lattice constant with the spin-orbit interaction included. The exchange splitting of Mn-3d bands is again prominent in the PLDOS of Fig. 6(c). Since the atomic number of Pt is larger than Mn, main peaks in PLDOS of Pt-5d bands appear at deeper energies than those of Mn-3d bands. Comparison between theory and experiment yields that calculated Pt-5d band widths agree well with those obtained from the PES experiment.[16] The total magnetic moment per formula unit is $4.00\mu_B$, which is again in good agreement with previous calculations and experiments.[18] The calculated magnetic moment at a Mn site is $3.97\mu_B$, and so the magnetic moment in PtMnSb is carried mainly

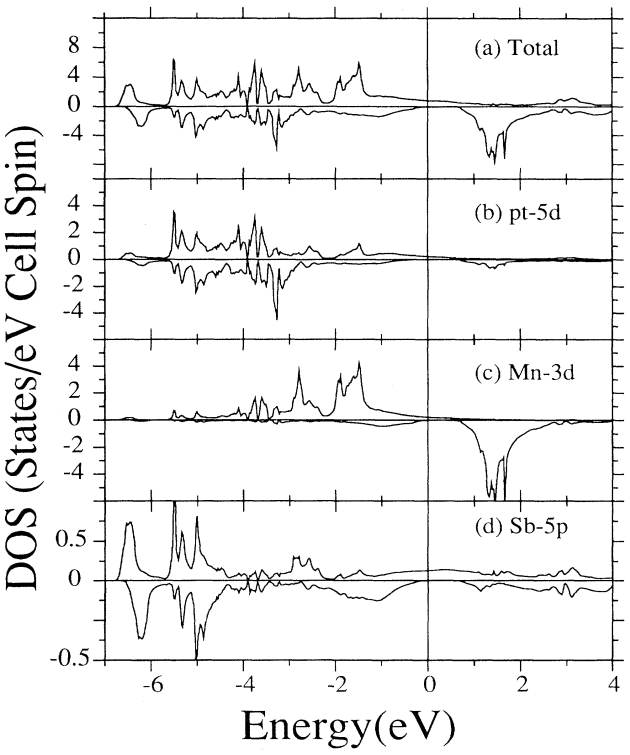

FIG. 6. The total DOS (states/eV spin cell) and PLDOS's (states/eV spin atom) of PtMnSb calculated at the experimental lattice constant. (a) Total DOS, (b) PLDOS of Mn-3d, (c) PLDOS of Pt-5d, and (d) PLDOS of Sb-5p.

TABLE IV. Occupied charges, Q_l, and magnetic moments, M, of ferromagnetic PtMnSb at the experimental lattice constant. The spin-orbit interaction is taken into account.

		Q_s	Q_p	Q_d	$Q_{\rm tot}$	M
Pt	↑	0.42	0.42	4.25	5.09	
	↓	0.42	0.49	4.10	5.01	0.08
Mn	↑	0.31	0.35	4.72	5.38	
	↓	0.26	0.30	0.85	1.41	3.97
Sb	↑	0.75	1.05	0.15	1.95	
	↓	0.74	1.15	0.15	2.04	−0.09
Empty	↑	0.19	0.27	0.12	0.58	
	↓	0.18	0.25	0.11	0.54	0.04

by Mn atoms, similarly as in NiMnSb (see Table IV). Pt atoms contribute little to the magnetic moment because the PLDOS of Pt-5d are nearly filled with electrons of both spin directions. In consequence, orbital polarizations originating from Pt atoms are canceled between majority and minority spin electrons, and thus total orbital contribution to the magnetic moment is as small as $0.08\mu_B$ in PtMnSb.

The spin-orbit effect on Fermi surfaces of PtMnSb is large. Figures 7(a) and 7(b) present Fermi surfaces of PtMnSb at the experimental lattice constant without and with the spin-orbit interaction included, respectively. The shape of the Fermi surface is similar to that of NiMnSb, except for the spin down components (dashed lines) near Γ. If the spin-orbit interaction is included, all the spin-down components disappear due to the half-metallic character, and the folded Fermi surfaces along the Γ-X direction are resolved.

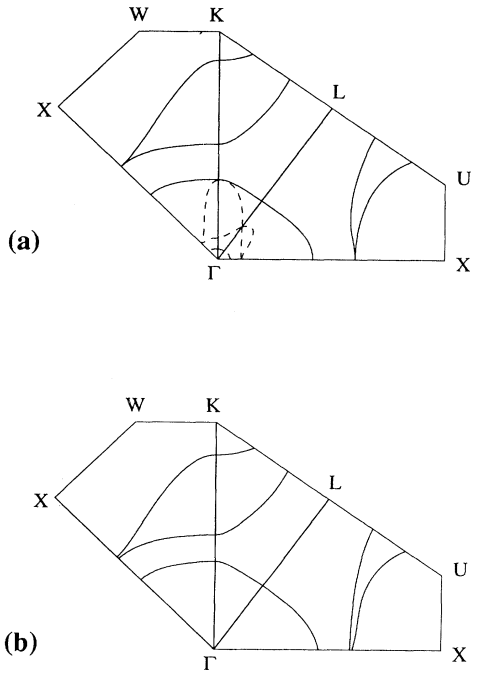

FIG. 7. Fermi surface cross sections of PtMnSb at the experimental lattice constant. (a) Semirelativistic calculation. Solid lines for spin-up and dotted lines for spin-down components. (b) Fermi surfaces with the spin-orbit interaction included.

V. FERROMAGNETIC COUPLING OF MAGNETIC MOMENTS

It has been suggested[18,22] that the couping of magnetic moments in Heusler compounds originates from the indirect Ruderman-Kittel-Kasuya-Yosida (RKKY) type interaction mediated by itinerant electrons. Based on this idea, one can identify the itinerant carriers responsible for the magnetic coupling as those on the nearly spherical hole Fermi surfaces of the 12th majority spin bands centered at Γ in NiMnSb and PtMnSb (see Figs. 3 and 7).[23] In the RKKY interaction, the exchange coupling parameter oscillates as a function of $2k_FR$, where k_F and R denote the Fermi wave vector and the distance between atoms, respectively. The mean radii (k_F's) of the Fermi surfaces of the 12th bands in NiMnSb and PtMnSb are small enough to couple magnetic moments of Mn atoms ferromagnetically. This is because $2k_FR_{M-M}$'s for NiMnSb and PtMnSb, 3.59 and 3.30, are smaller than the first node of the RKKY oscillatory function ($2k_FR = 4.49$). Here R_{M-M} is the nearest neighbor distance between Mn atoms. Hence, the exchange coupling parameters between Mn magnetic moments become positive (ferromagnetic) for both NiMnSb and PtMnSb.

Our band results indicate that the itinerant electrons that mediate RKKY interaction consist of not only wide Sb-p band electrons, but also Ni-d or Pt-d band electrons. Sb-p holes exist mostly at the center of the Fermi sea of the 12th band, but decrease as going toward the Fermi surface. Near the Fermi surface, the percentile fraction of electrons in NiMnSb is 43, 21, 10, 9% for Ni-3d, Mn-3d, Sb-5p, and Sb-5s, respectively. Since the RKKY interaction is mediated by electrons near the Fermi surface, Ni-d electrons are expected to play an important role in constructing ferromagnetic couplings between magnetic moments at Mn sites. Pt-d electrons in PtMnSb will play a similar role, since the percentile fraction of electrons near the Fermi surface of PtMnSb is 27, 24, 17, 8% for Pt-5d, Mn-3d, Sb-5s, and Sb-5p, respectively. In PtMnSb, there are more Sb-5s electrons than Sb-5p near the Fermi surface, which is different from the case of NiMnSb. Note that, in both cases, there are some of itinerant Mn-d electrons near the Fermi surface, which may take part in the RKKY interaction.

Otto *et al.*[18] have speculated that the low T_C in AuMnSb results from the fact that one more electron than in PtMnSb fills up the itinerant holes of Sb-5p band and so there are not enough carriers to mediate an interaction. To test this, we have performed the band calculation on AuMnSb.[24] Our calculation yields that the Γ-centered hole Fermi surface of the 12th majority spin band disappears completely, but there appear new hole Fermi surfaces of the 13th and 14th spin-up bands centered at Γ and an electron Fermi surface of the 15th spin-up band centered at X. The existence of new Fermi surfaces indicates that the number of itinerant carriers in AuMnSb is not so small, as compared to the case in

NiMnSb or PtMnSb. Therefore, we think that the low T_C of AuMnSb is caused by a weaker hybridization interaction between Mn-d and Au-d electrons than that between Mn-d and Pt-d electrons, because the Au-d band, which is located deeper in energy, does not overlap much with the Mn-d band. Weaker hybridization gives rise to a smaller RKKY interaction, and concomitantly a low T_C. This seems to be consistent with the above finding that the mediating electrons are not only Sb-5p electrons but also Ni-d or Pt-d electrons.

VI. CONCLUSION

We have performed total energy LMTO band calculations for both NiMnSb and PtMnSb. Equilibrium lattice constants obtained in the ferromagnetic calculations agree very well with experimental values within errors of 0.3% for NiMnSb and 0.5% for PtMnSb. Semirelativistic band structure calculations yield half-metallic NiMnSb at the experimental lattice constant. Meanwhile, PtMnSb is a normal-metal in the semirelativistic calculation but becomes a half-metal if the spin-orbit interaction is explicitly taken into account. The magnitudes of the energy gap in the minority spin bands are found to be sensitive to the variation of the lattice constant for both NiMnSb and PtMnSb.

Effects of the spin-orbit interaction on band structures and Fermi surfaces are found to be substantial in PtMnSb, but negligible in NiMnSb. In PtMnSb, the large spin-orbit splitting of the bands at Γ near E_F is mainly attributed to Pt-6p bands with minority spin-down characters, which play an important role in the optical transition to give rise to an enhanced MOKE. It is also found that the itinerant electrons, that mediate RKKY interaction between Mn magnetic moments in NiMnSb and PtMnSb, are those on the nearly spherical hole Fermi surfaces of the 12th majority spin bands centered at Γ, and they consist of not only wide Sb-p band electrons but also Ni-d or Pt-d band electrons.

ACKNOWLEDGMENTS

Helpful discussions with J.-S. Kang are greatly appreciated. This work was supported by the POSTECH-BSRI program of the Korean Ministry of Education.

[1] R. A. de Groot and F. M. Mueller, P. G. van Engen, and K. H. J. Buschow, Phys. Rev. Lett. **50**, 2024 (1983).
[2] P. G. van Engen, K. H. J. Buschow, R. Jongebreur, and M. Erman, Appl. Phys. Lett. **42**, 202 (1983).
[3] R. A. de Groot, F. M. Mueller, P. G. van Engen, and K. H. J. Buschow, J. Appl. Phys. **55**, 2151 (1984).
[4] R. A. de Groot, P. G. van Engen, P. P. J. van Engelen, and K. H. J. Buschow, J. Magn. Magn. Mater. **86**, 326 (1990).
[5] K. E. H. M Hanssen and P. E. Mijnarends, Phys. Rev. B **34**, 5009 (1986).
[6] E. Kulatov and I. I. Mazin, J. Phys. Condens. Matter **2**, 343 (1990).
[7] O. K. Andersen, Phys. Rev. B **12**, 3060 (1975).
[8] U. von Barth and L. Hedin, J. Phys. C **5**, 1629 (1972).
[9] In LMTO-ASA band calculations for compound materials, there is always an ambiguity in choosing an atomic sphere radius of each element. In our case, we chose the same atomic radii, since covalent radii of the elements are not much different (the covalent radius of Sb is slightly larger than that of Ni or Mn). The test calculation for NiMnSb with different atomic sphere radii, where the ratio of radii for Ni, Mn, Sb, and empty sphere is 1.0:1.0:1.1:0.5 as employed Ref. 6, yields nearly the same electronic structures as those of Fig. 1. In both cases, there are substantial Sb-d characters which arise from tail parts of near neighbor wave functions, and so it is necessary to include Sb-d orbital in the LMTO basis.
[10] O. Jepsen and O. K. Andersen, Solid State Commun. **9**, 1763 (1971).
[11] B. I. Min and Y.-R. Jang, J. Phys. Condens. Matter **3**, 5131 (1991).
[12] F. Heusler, Verh. Dtsch. Phys. Ges. **5**, 219 (1903).
[13] The packing ratio of C_{1b} structure is 51%, which is slightly smaller than that of simple cubic structure (52.4%).
[14] J. F. Janak, Phys. Rev. B **16**, 255 (1977).
[15] P. A. M. van der Heide, W. Baelde, R. A. de Groot, A. R. de Vroomen, P. G. van Engen, and K. H. J. Buschow, J. Phys. F **15**, L75 (1985).
[16] J.-S. Kang, J. H. Hong, S. W. Jung, Y. P. Lee, J.-G. Park, C. G. Olson, S. J. Youn, and B. I. Min, Solid State Commun. **88**, 653 (1993).
[17] R. B. Helmholdt, R. A. de Groot, F. M. Müller, P. G. van Engen, and K. H. J. Buschow, J. Magn. Magn. Mater. **43**, 249 (1984).
[18] M. J. Otto, H. Feil, R. A. M. Van Woerden, J. Wijngaard, P. J. Van Der Valk, C. F. Van Bruggen, and C. Haas, J. Magn. Magn. Mater. **70**, 33 (1987).
[19] The type of the exchange-correlation interaction and atomic sphere radii employed by de Groot *et al.* were not specified in Refs. 1 and 3. Only in the work by Wijngaard, Haas, and de Groot [Phys. Rev. B **40**, 9318 (1989)] was it mentioned that the local density approximation of Hedin and Lundqvist was used. The band structure of PtMnSb in this work, however, does not seem to be exactly the same as that given in Ref. 3.
[20] J. L. Erskin and E. A. Stern, Phys. Rev. B **8**, 1239 (1973).
[21] In comparison, the range of the lattice constant, where NiMnSb is half metallic, is between 5.87 Å and 6.09 Å.
[22] J. Kübler, A. R. Williams, and C. B. Sommers, Phys. Rev. B **28**, 1745 (1983), and references therein.
[23] The RKKY interaction is characterized by the Fermi wave vector, k_F, which is the radius of a closed spherical Fermi surface. Γ-centered hole pockets are only spherical Fermi surfaces existing in NiMnSb and PtMnSb, and thus it is assumed that itinerant electrons mediating RKKY interaction are from these pockets. Note that other Fermi surfaces are all open orbits.
[24] S. J. Youn and B. I. Min (unpublished).